

Modeling and Analysis of Anechoic Chamber Using CEM Tools

D. Campbell¹, G. Gampala¹, C. J. Reddy¹, M. Winebrand², and J. Aubin²

¹EM Software & Systems (USA), Inc.
100 Exploration Way, Suite 300, Hampton, VA 23666
derek@emssusa.com

²ORBIT/FR, Inc.
506 Prudential Road, Horsham, PA 19044
JohnA@OrbitFR.com

Abstract—Advances in computational resources facilitate anechoic chamber modeling and analysis at VHF/UHF frequencies using full-wave solvers available in commercial software such as FEKO. The measurement community has a substantial and increasing interest in utilizing computational electromagnetic (CEM) tools to minimize the financial and real estate resources required to design and construct a custom anechoic chamber without sacrificing performance. A full-wave simulation analysis such as the finite element method (FEM) provides a more accurate solution than the approximations inherent to asymptotic ray-tracing techniques such as physical optics (PO), which have traditionally been exploited to overcome computational resource limitations. An anechoic chamber is simulated with a rectangular down-range cross-section (in contrast with the traditional square cross-section) to utilize the software's capability to assess polarization performance. The absorber layout within the anechoic chamber can be optimized using FEKO for minimal reflections and an acceptable axial ratio in the quiet zone. Numerical results of quiet zone disturbances and axial ratios are included for both low- and medium-gain source antennas over a broad frequency range.

Index Terms - Anechoic chamber, axial ratio, computational electromagnetics, FEKO, finite element method, and physicaloptics.

I. INTRODUCTION

The optimum choice of anechoic chamber dimensions is crucial to ensure the minimum performance level of the quiet zone and to minimize the system cost. In many cases, however, the dimensions are predetermined (e.g., rectangular rather than square cross-section). The chamber geometry is not the only parameter limiting quiet zone performance. The quiet zone behavior depends on several factors such as absorbing material performance, layout and grades, source antenna/device under test (DUT) separation, source antenna beamwidth, DUT positioning equipment geometry and material, *etc.* A full 3D electromagnetic analysis must be performed to correctly account for all of these parameters.

To date, the industry most often analyzes anechoic chambers with a method similar to “ray tracing”, which suffers from poor accuracy. The inaccuracy is especially prevalent in scenarios where the room characteristic dimensions are only a few wavelengths (i.e., a typical situation at VHF/UHF frequency bands). A few components contributing to the inaccuracy are detailed below:

- Limited data is available on the reflectivity of absorbing materials at VHF/UHF, especially at off-normal incidence. Historically, the reflection coefficient is only described by magnitude and the phase is not provided. As a result, only approximate information can be extracted from the RMS fields in the quiet zone. In some cases, assumptions were made on the reflectivity at off-normal incidence

angles at VHF/UHF frequencies based on similarities to better established reflectivity curves at higher frequencies (e.g., >2.0GHz). However, the extrapolation has been proven inaccurate for a number of VHF/UHF chambers. In other cases, the off-normal incidence data is retrieved from normal incidence reflectivity using Fresnel formulas, which are accurate for planar absorbing multi-layered structures only.

- Specular area characteristic dimensions include a few wavelengths of surface covered by absorbing material (e.g., pyramids, wedges, etc.), which at VHF/UHF may exceed side wall characteristic dimensions and may, therefore, span a large range of incidence angles of the illuminating rays on the specular area. Choosing the correct incidence angle and corresponding reflection coefficient at each consecutive specular point then becomes a difficult process. Upgrading the “ray-tracing” method to the “aperture integration” method is a better fit for the analysis. However, accuracy is limited by the data available for the reflectivity of absorbing materials.

Thus, the need for a more rigorous and comprehensive analysis such as a full 3D electromagnetic simulation is obvious, especially at VHF/UHF bands [1, 2]. Insufficient accuracy in the chamber design has resulted in some poor chamber implementations in the past. Even identifying improper chamber performance with the VSWR test procedure is a difficult process at VHF/UHF bands. The test may show uniform field distribution in the quiet zone, while the overall chamber performance is far from optimal.

Some factors limiting the effectiveness and accuracy of the VSWR tests for chamber certification at the VHF/UHF bands are:

- Often the test zone dimensions are comparable to or less than 1λ at the lowest operating frequency. Thus, visually retrieving and/or distinguishing the ripples (period and ripple amplitude) associated with multiple reflections in the chamber interior to the fullest extent from the measured data are part of a difficult process. The chamber may even appear to achieve acceptable performance in scenarios where the reflected signal is stronger than the direct (desired) one.

- Due to geometry constraints the field probe antenna used in the free-space, VSWR procedure is typically a low- or medium-gain antenna. In cases with relatively high reflections in the shielded room, the reference measurement results may be in error. An uncertainty is then added through the entire VSWR data processing. Consequently, there could be a situation at VHF/UHF bands where the VSWR tests optimistically report the quiet zone reflectivity performance.
- The VSWR procedure is often inapplicable without modifications (e.g., transversal cuts in elongated chambers such as tapered ones). As a result, the procedure is frequently “engineered” to exclude conflicting/confusing measurement data.

The primary manifestation of a poor elongated chamber performance includes:

- Inconsistent longitudinal trace behavior in the quiet zone over a broad frequency range.
- Significant signal level variation over a broad frequency range with the source and probe antennas rotated simultaneously (clocked) around their boresight (the chamber line of sight).

In order to assure that the chamber performs well, a significant amount of extra testing is required to be performed on the quiet zone, which might be costly or often impossible to execute. Effort has previously demonstrated an efficient method for modeling the reflectivity of absorber, while saving computational resources as compared to a full 3D EM solver [3].

A full 3D anechoic chamber simulation at VHF/UHF frequencies is a helpful tool that may be used to predict/estimate some test results and assure optimal performance. In particular, 3D anechoic chamber simulations can estimate the axial ratio accuracy, which can be achieved in the chamber with a non-square cross-section.

II. NUMERICAL METHODS

As computational resources such as memory and processors continue to experience reductions in price, state of the art CEM techniques available in commercial software packages such as FEKO [4] are becoming a more attractive option for engineers during the design phase of anechoic chambers. Full-wave techniques, such as finite-

difference time-domain (FDTD), method of moments (MoM), multi-level fast multipole method (MLFMM), and finite element method (FEM) accurately solve Maxwell's equations without approximations and are therefore becoming a popular choice with the availability of cheaper memory and CPU power. To demonstrate feasibility of anechoic chamber design at VHF/UHF frequencies using a full-wave technique such as FEM, we chose the commercial EM simulation tool FEKO.

FEKO is a comprehensive electromagnetic software suite that includes asymptotic solvers such as physical optics (PO), geometrical optics (GO), and uniform theory of diffraction (UTD) together with the full-wave solvers including MoM, MLFMM, and FEM. The asymptotic methods and FEM have been hybridized with MoM to assist with solving large and complex problems [5-7]. Asymptotic methods are well suited for the analysis of electrically large anechoic chambers. Apart from providing a solution with limited resources, asymptotic methods operate with underlying approximations wherein vigilance is required to model the problem well within those approximations.

In this paper, the analysis and design process for an anechoic chamber is presented. The design process utilizes both the full-wave FEM and asymptotic PO techniques, which are ideal for this electrically large, non-radiating dielectric model. FEM utilizes a volume meshing technique that employs tetrahedral elements to accurately mesh arbitrarily shaped volumes where the dielectric properties may vary between neighboring tetrahedral elements. The outer shell is meshed with triangular elements and does not require a radiation boundary. In contrast, PO utilizes a surface meshing technique that employs triangular elements to accurately mesh arbitrarily shaped surfaces where the dielectric properties are homogeneous.

III. CHAMBER AND ANTENNA MODELING

A custom anechoic chamber with a rectangular down-range cross-section (i.e., $W \times H$) is modeled to fit within a physically limited volume. FEM was used to analyze an anechoic chamber model with a perfectly conducting outer

shell. The chamber dimensions are 17" H \times 24" W \times 32.5" L as shown in Fig. 1, where the orange color represents the outer shell modeled as PEC and the blue represents the inner absorbing material.

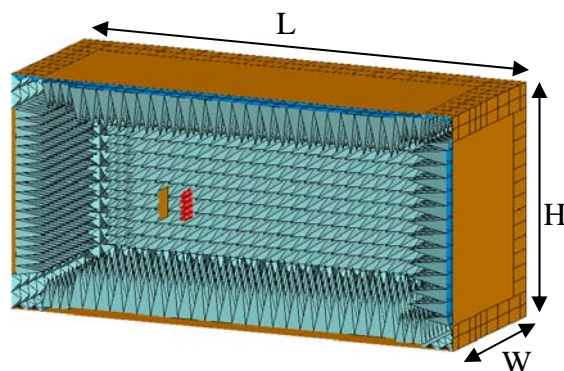


Fig. 1. Anechoic chamber model dimensions.

The center of the quiet zone is 10" from the receiving wall and measures 6" H \times 6" W \times 6" L. The source antenna is modeled at a 10" separation from the center of the quiet zone (i.e., 20" from the receiving wall) and visible left of center in Fig. 1. PO was employed to analyze an anechoic chamber model with a dielectric shell as shown in Fig. 2, because FEKO limits the analysis with PO to a single material within a given model.

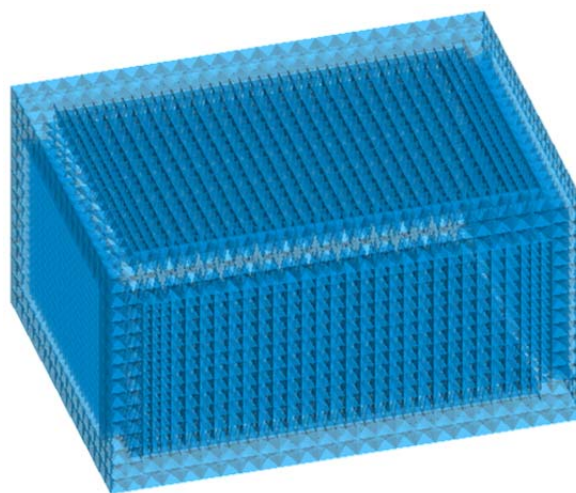


Fig. 2. Anechoic chamber analyzed with PO.

Both low- and medium-gain source antennas are modeled for vertical and horizontal polarizations with a directive gain of ~ 6 and 10 dBi, respectively. Any type of source antenna can be included in the model. For practical reasons, we

have chosen to generate a source antenna, similar to Fig. 3, with 25 current sources measuring $\lambda/15$ in length and arranged on a plane to achieve the desired beam widths in both the E- and H-planes, where λ is the operating wavelength. A realistic pattern is emulated by minimizing the energy radiating toward the rear of the chamber with a PEC reflector separated by $\lambda/4$ (represented by orange).

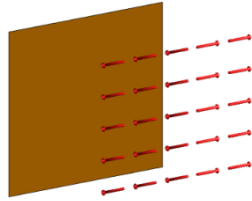


Fig. 3. Source antenna model used for analysis.

The 3dB beam widths (BW) of the source antennas are summarized below in Table II.

Table I: Source antenna of 3 dB BW.

Gain	E-Plane 3dB BW	H-Plane 3dB BW
Low	68°	111°
Medium	65°	67°

A center patch region of the two side walls, the receiving wall, the floor and ceiling were modeled with large pyramidal absorber and surrounded by small pyramidal absorber as illustrated in Fig. 4.

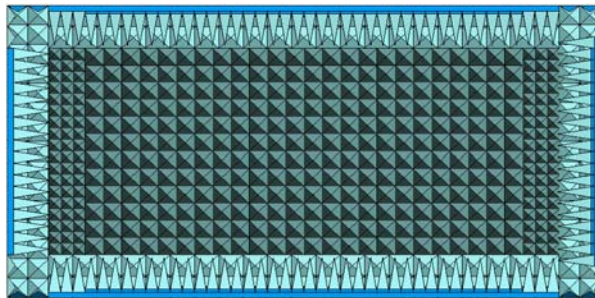


Fig. 4. Large absorber was used in center patch region of several walls.

The large pyramidal absorber is modeled with a 12" H \times 12" W \times 6" L cuboid base below a 36" long pyramid. The small pyramidal absorber in the surrounding area is modeled with an 8" H \times 8" W \times 4" L cuboid base below a 24" long pyramid as shown in Fig. 5.



Fig. 5. Large and small pyramidal absorber models.

The real and imaginary dielectric constant for the absorbing material is illustrated in Fig. 6 and 7, respectively. The upper line indicates the maximum value, the lower line indicates the minimum value and the middle solid line indicates the average dielectric constant resulting from the manufacturing tolerances.

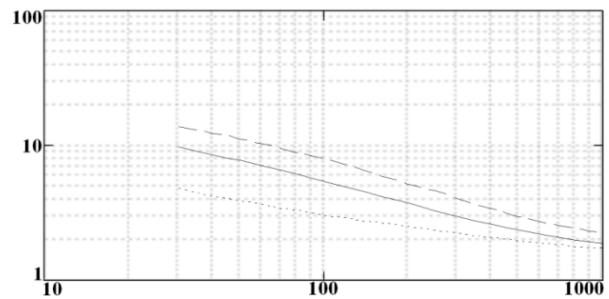


Fig. 6. Real dielectric constant for the absorber.

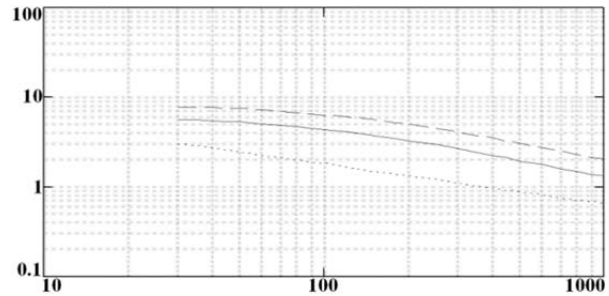


Fig. 7. Imaginary dielectric constant for the absorber.

We have elected to use the average dielectric constant and loss tangent for the absorber as summarized below in Table II for the frequencies analyzed.

Table II: Absorber material properties.

Frequency	ϵ'_r	ϵ''_r	Tan δ
150 MHz	4.758	4.467	0.93884
250 MHz	3.5	3.0	0.85714
500 MHz	2.4	1.95	0.81250
1000 MHz	1.95	1.4	0.71795
2000 MHz	1.95	1.4	0.71795

The computer memory required depends on the size of the mesh (i.e., number of tetrahedra and/or triangles), dielectric constant, and frequency as summarized in Table III and IV.

Table III: FEM mesh characterization.

Frequency	Tetrahedra	Triangles	Memory
150 MHz	1181640	43508	14 GB
250 MHz	3265760	86404	43 GB
500 MHz	12 583 444	234 684	196 GB

Table IV: PO mesh characterization.

Frequency	Triangles	Memory
500 MHz	2 364 916	10 GB
1000 MHz	7 615 698	31 GB
2000 MHz	30 035 292	123 GB

The respective run times required for this model are listed in Table V.

Table V: Simulation runtime.

Frequency	Method	Run Time
150 MHz	FEM	3 min
250 MHz	FEM	12 min
500 MHz	FEM	81 min
500 MHz	PO	27 min
1000 MHz	PO	77 min
2000 MHz	PO	271 min

Simulations were performed on a workstation with an Intel Xeon E5-2650 CPU with a total of 8 processors operating at 2.0 GHz. The workstation had 256 GB of shared memory available.

IV. ERROR ANALYSIS

Numerical results are computed for both the down-range cross-section of the fields in the center of the quiet zone and the down-range axial ratio. The quiet zone fields were then normalized with fields produced by an identical antenna radiating into free space. This process was repeated for two distinct frequencies (i.e., 150 MHz and 250 MHz). The normalized fields represent an error term produced by energy reflecting off of the absorber,

$$\varepsilon = \left| 20 \log \sqrt{\frac{\sum |Chamber Field Components|^2}{\sum |Clear Site Field Components|^2}} \right|. \quad (1)$$

The down-range axial ratio, quantifies the polarization performance of an anechoic chamber by comparing the results from a simulation using a

horizontally polarized antenna to the results from a simulation using a vertically polarized antenna,

$$AR = \left| 20 \log \sqrt{\frac{\sum |H Pol Field Components|^2}{\sum |V Pol Field Components|^2}} \right|. \quad (2)$$

These two equations help quantitatively validate the performance of a custom anechoic chamber configuration.

V. RESULTS

The errors produced in the central cross-section of the quiet zone have been analyzed with equation (1) for both low- and medium-gain source antennas for horizontal and vertical polarizations.

Fig. 8, 9, and 10 illustrate the results for a horizontally polarized, low-gain source antenna operating at 150 MHz, 250 MHz, and 500 MHz, respectively. The vertically polarized data sets were omitted for brevity. Fig. 11 and 12 depict the error produced when operating at 150 MHz and 250 MHz, respectively, for a vertically polarized, medium-gain source antenna. The horizontally polarized data sets were omitted for brevity.

Note the collection of plots in Fig. 8 through Fig. 12 illustrates a quiet zone error generally below 1 dB. Fig. 13 illustrates the axial ratio error from equation (2) along the length of the anechoic chamber through the center of the quiet zone for low- and medium-gain source antennas operating at 150 MHz and 250 MHz.

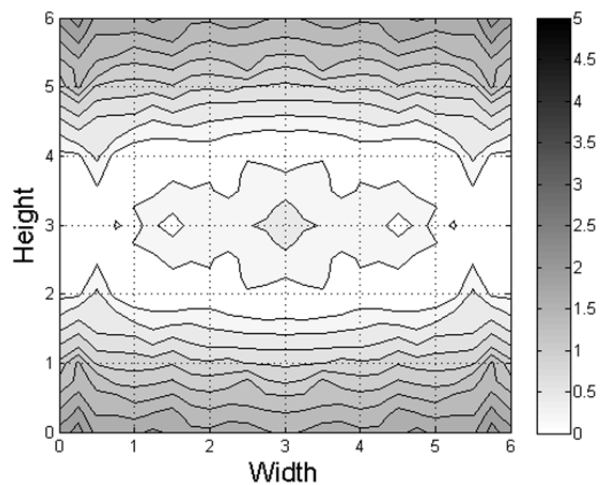


Fig. 8. Error when operating an H-polarized low-gain source antenna at 150 MHz.

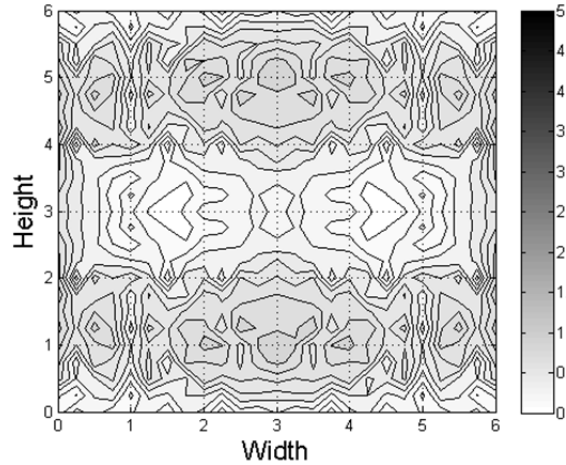


Fig. 9. Error when operating an H-polarized low-gain source antenna at 250 MHz.

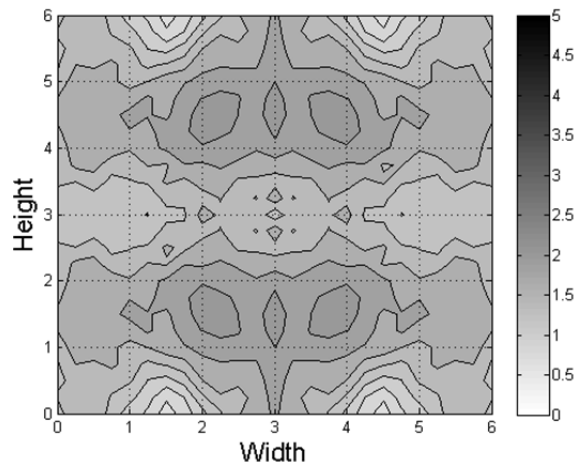


Fig. 10. Error when operating an H-polarized low-gain source antenna at 500 MHz.

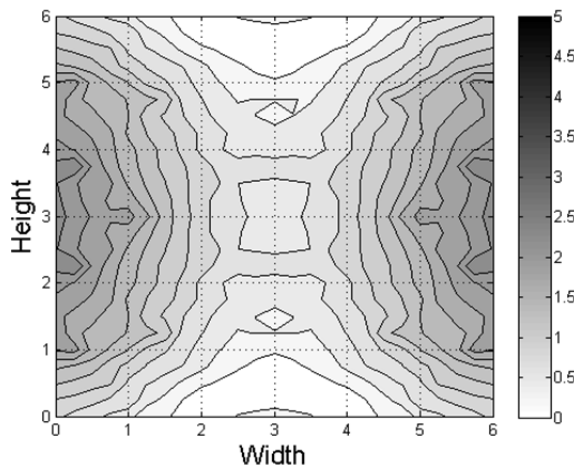


Fig. 11. Error when operating a V-polarized medium-gain source antenna at 150 MHz.

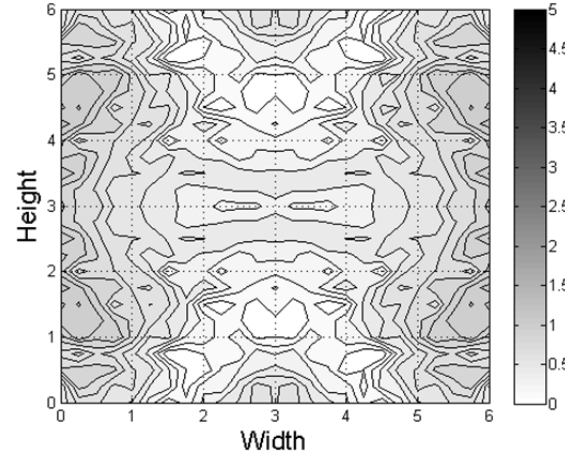


Fig. 12. Error when operating a V-polarized medium-gain source antenna at 250 MHz.

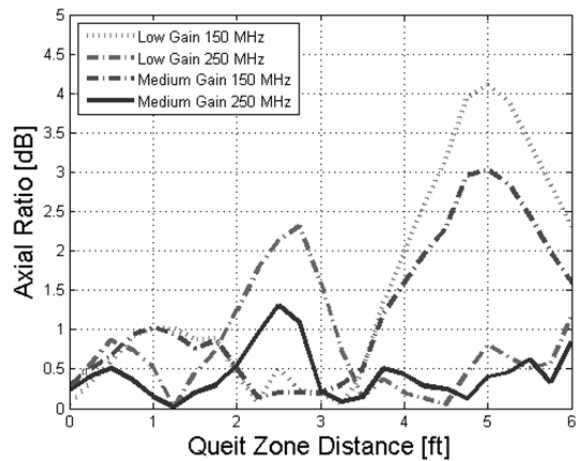


Fig. 13. Axial ratio for low- and medium-gain source antennas operating at 150 and 250 MHz.

Note the behavior of the curves in Fig. 13 is largely explained by the rectangular cross-section of the chamber resulting in:

- Different reflectivity exhibited by the side walls, the floor, and the ceiling.
- Different free space attenuation associated with different propagation distance of the reflected waves from the side walls and the floor and ceiling to the center of the quiet zone.

In theory, the axial ratio does not exist in a symmetrical chamber with a squared cross-section. If detected in a practical squared cross-section chamber, the axial ratio error is associated only with the manufacturing tolerances contributing to the error.

In addition to analyzing the anechoic chamber with FEM, the PO technique was also validated by comparing near fields in the quiet zone when operating at 500 MHz. The difference between the FEM and PO results is illustrated in Fig.14.

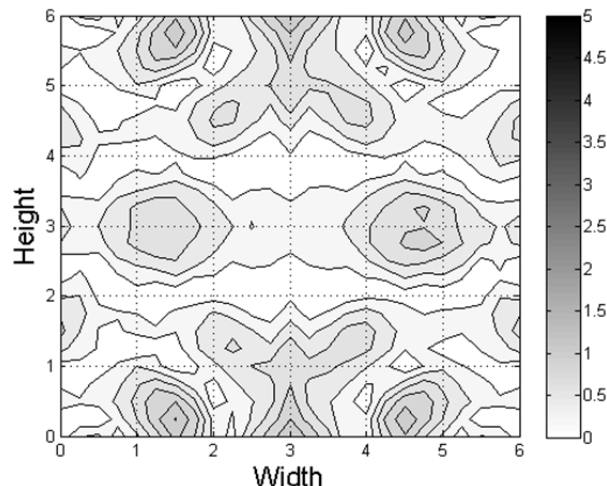


Fig.14. The difference between FEM and PO analysis results when operating at 500 MHz.

The PO technique is shown to have a maximum error of 1.0 dB when computing near fields in the quiet zone of an anechoic chamber. The additional error introduced by the physical optics method is limited, which facilitates simulating the anechoic chamber at much higher frequencies. As shown in Table IV and V, we simulated the anechoic chamber up to 2 GHz. Further increases in frequency are possible.

VI. CONCLUSION

Both full-wave and asymptotic analyses have been performed on the quiet zone of a rectangular cross-section anechoic chamber at VHF/UHF frequencies using a 3D solver within the FEKO simulation software. The results demonstrate meaningful and expected performance in the chamber with rectangular cross-section, which indicate that:

- Quiet zone performance (reflectivity) is improving as operating frequency increases.
- Quiet zone performance degrades with the increasing separation between the source antenna and quiet zone.
- A higher gain source antenna provides better quiet zone performance.

- The linear rotating polarization axial ratio is getting worse with longer separation between the source antenna and the quiet zone.
- Axial ratio is improving at higher frequencies.
- Axial ratio is improving for a higher gain source antenna.

FEKO is an effective tool for performing computational analyses of anechoic chambers at VHF/UHF frequency bands. Of particular value is the fact that one can switch from a rigorous method like FEM to an asymptotic method like PO within the same environment. Future applications of the FEKO simulation software to assist with analyzing anechoic chambers are expected.

REFERENCES

- [1] M. Winebrand and J. Aubin, "Test zone performance in low frequency anechoic chambers," *Proceeding of the AMTA*, pp. 482-486, 2008.
- [2] M. Winebrand and J. Aubin, "Low frequency 3-D electromagnetic analysis of anechoic chamber performance," *Microwave Journal*, October 2008.
- [3] M. Agatonovic, Z. Marinkovic, and V. Markovic, "Application of ANNs in evaluation of microwave pyramidal absorber performance," *Applied Comp. Electro. Society (ACES) Journal*, vol. 27, no. 4, Apr. 2012.
- [4] FEKO Suite 6.1, EM Software and Systems, 2011. www.feko.info
- [5] U. Jakobus and F. M. Landstorfer, "Improved PO-MM hybrid formulation for scattering from three-dimensional perfectly conducting bodies of arbitrary shape," *IEEE Transactions on Antennas and Propagation*, vol. 43, pp. 162-169, Feb. 1995.
- [6] I. P. Theron, D. B. Davidson, and U. Jakobus, "Hybridization of the method of moments with a UTD treatment of a conducting cylinder," *Proceedings of the 8th Biennial IEEE Conference on Electromagnetic Field Computation, CEFC'98, Tucson*, pp. 107, June 1998.
- [7] M. Bingle, J. Tonder, and U. Jakobus, "Acceleration of the hybrid FEM/MoM technology in FEKO with the multilevel fast multipole method," *The 10th International Workshop on Finite Elements for Microwave Engineering*, Oct. 2010.



Derek D. Campbell was born in Marion, IN on July 23, 1983. He received the B.S. and M.S. degrees in Electrical Engineering from the Georgia Institute of Technology in 2006 and 2011, respectively. From 2002 to 2011 he served as a Research Engineer at the Georgia Tech Research Institute where he performed RCS and antenna measurements as well as analyzed geolocation algorithms. In 2012, he joined EM Software & Systems (USA) as an Application Engineer. His current interests are in the areas of electromagnetic theory and numerical methods primarily applied to antennas and scattering.



Gopinath Gampala joined EM Software & Systems (USA), Inc. as an Application Engineer in 2008 and was promoted to Senior Application Engineer in November 2012. Mr. Gampala has a B.S. degree in Electronics and Communications Engineering from the Jawaharlal Nehru Technological University, Hyderabad, India. The topic of his research for his Master's degree, which he obtained from the University of Mississippi, was "Analysis and Design of Artificial Magnetic Conductors for X-Band Antenna Applications." He has experience in numerical methods for electromagnetics and during the past five years he focused on compact antenna designs using high impedance ground planes and MIMO antenna designs for LTE/4G handsets.



C. J. Reddy received M.Tech. degree in Microwave and Optical Communication Engineering and PhD in Electrical Engineering from the Indian Institute of Technology, Kharagpur, India, in 1986 and 1988, respectively. In 1991, he was awarded an NSERC Visiting Fellowship to conduct research at the Communications Research Center, Ottawa, Canada. In 1993, he was awarded a National Research Council (USA) Research Associate position to conduct research in computational electromagnetics at NASA Langley Research Center, Hampton, Virginia. Currently, Dr. Reddy is the President and Chief Technical Officer of Applied EM Inc., a small company specializing in computational electromagnetics, antenna design, and development. At Applied EM, Dr. Reddy successfully led many small business innovative research (SBIR) projects from the US Department of Defense (DoD). Dr. Reddy also serves as the President of EM Software &

Systems (USA) Inc. At EMSS (USA), he is leading the marketing and support of the commercial three-dimensional electromagnetic software *FEKO* in North America. Dr. Reddy is a Senior Member of the IEEE and a Senior Member of the Antenna Measurement Techniques Association (AMTA). He is a Fellow of the Applied Computational Electromagnetic Society (ACES), and served as a member of its Board of Directors. He has published 35 journal papers, 54 conference papers, and 17 NASA Technical Reports to date. Dr. Reddy was the General Chair of the ACES 2011 and 2013 conferences.



John Aubin currently serves as Vice President for Engineering and also as Chief Technology Officer at ORBIT/FR Inc. in Horsham, PA. Mr. Aubin received the BSEE from Virginia Tech in 1977, MBA from Temple University in 1983, and MSEE from Drexel University in 1988. He has previously been engaged in the design and implementation of high performance earth station antennas and beam waveguide systems, EW and radar antennas, monopulse tracking radars, and broadband horn antennas in addition to his work in automated antenna and RCS measurement systems. His current interests include antenna and radar cross section measurement technology, wireless systems, radar and microwave systems engineering, and antenna design. Mr. Aubin has served as principal design engineer on a number of automated antenna and radar measurement systems ranging from VHF up to millimeter waves, including a microwave imaging system for evaluation of biological tissue, a high performance low frequency radar cross section measurement system, and a dynamic radar cross section measurement system using an integrated tracking and signature measurement radar. Mr. Aubin has authored over 40 papers on antennas, radar, and measurement technology.